Fine-Scale Bacterial Community and Chemical Changes within Steel Corrosion Tubercles in the Duluth-Superior Harbor

A thesis submitted to the faculty of the graduate school of the University of Minnesota

By

Jo Jo Aunastaushia Thomas

In partial fulfillment of the requirements for the degree of Master of Science

Adviser: Randall E. Hicks

October 2016

Acknowledgements

I would like to first acknowledge my advisor, Dr. Randall Hicks. Dr. Hicks is an excellent mentor and ensured that I developed the skills necessary to be successful in the professional world. He allowed me to work independently while still being available to guide me when necessary. Dr. Hicks uses his tremendous experience and knowledge to train each of his students to be mindful, professional scientists. I would also like to thank the members of my committee- Dr. Richard Axler, Dr. Nathan Johnson and Dr. Michael Sadowsky for sharing their time and expertise.

I would like to thank the other members of the Hicks laboratory for all their help. Dr. Drew Reed was instrumental in the methods development for this work and his assistance with the sampling and microbial work was indispensable. Caitlin Sloan and Wendy Zhao helped on sampling days, trained me on new techniques and provided a great working environment. I would also like to thank undergraduate Ryan Armstrong for his work on the electrochemical measurements and Dr. Chris Staley for his instruction on analyzing Illumina sequencing data.

Chad Scott and AMI Consulting Engineers, Superior, WI were essential for the manufacturing, placement and recovery of steel sample coupons. Thank you, also, to Ricky Ray at the Naval Research Laboratory, Stennis Space Center for his work to profile corrosion pits.

This work is the result of research sponsored by the Minnesota Sea Grant College Program supported by the NOAA office of Sea Grant, United States Department of Commerce, under grant No. EFS#00014434 (Sea Grant Research Project: R/CC-03-12). The U.S. Government is authorized to reproduce and distribute reprints for government purposes, notwithstanding any copyright notation that may appear hereon. Support was also received from the University of Minnesota Duluth, Department of Biology through teaching assistantships and travel grants from the Integrated Biosciences graduate program, the Swenson College of Science and Engineering and the University of Minnesota Graduate School. Without the support of these organizations this work would not have been possible.

Dedication

This thesis is dedicated to Dr. Drew Reed, who taught me about far more than just steel corrosion and research work. His advice and guidance will stay with me for my entire career and his laughter and spirit will live on in my memory.

Abstract

Corrosion of steel structures in the Duluth-Superior Harbor (DSH) is a severe economic problem. This corrosion is characterized by deep pits covered by crusty, orange, blister-like structures called tubercles. Prior research demonstrated these tubercles contain both iron-oxidizing (IOB) and sulfate-reducing bacteria (SRB) but fine scale changes of bacterial community structure within these tubercles remain unknown. Experimental steel coupons were placed at four sites in the DSH in 2006 and 2012 and recovered in 2013 to measure chemical gradients and identify bacteria associated with young and old corrosion tubercles. Oxygen concentrations measured with microelectrodes decreased from saturation in the overlying water to nearly anoxic conditions at the surface of tubercles while ferrous iron (Fe^{2+}) concentration increased with depth inside the tubercles. Bacterial DNA from different regions of the tubercles was sequenced using a next-generation sequencing technique to characterize the bacterial communities. Bacterial community composition changed within the tubercles. Families containing bacteria that oxidize iron and sulfur were consistently found on the outsides of tubercles and on non-tubercle steel. Families with bacteria that reduce iron and sulfur were found on the undersides of tubercles and in corrosion pits on the steel surface. Iron-oxidizing bacteria were more abundant after 0.8 years than 6.6 years and were distributed throughout tubercles while sulfate-reducing bacteria were most abundant in corrosion pits. Combined, these data are consistent with the cathodic depolarization (differential aeration cell model) and direct electron transfer theories of pitting corrosion, which provide explanations for the roles of bacteria in the accelerated corrosion of steel structures.

Table of Contents

Acknowledgements	i
Dedication	iii
Abstract	iv
Table of Contents	v
List of Tables	vi
List of Figures	vii
List of Abbreviations	viii
Introduction	1
Methods	8
Site locations and sample collection	8
Water chemistry	11
Corrosion pit depths	12
Microelectrode analysis	12
Microbial community sampling and analysis	14
Results	21
Water chemistry	21
Corrosion pit depths	21
Microelectrode analysis	25
Microbial community differences	28
Discussion	39
References	48

List of Tables

Table 1.	Sulfate, chloride, total alkalinity and total copper measured in water and Larson-Skold Index at four sites in the St. Louis River Estuary during June 2013	22
Table 2.	Bacterial families that had higher relative abundances in different corrosion tubercle zones on corroding steel coupons after 0.8 and 6.6 years of exposure at four sites in the St. Louis River Estuary	34
Table 3.	Bacterial families contributing at least 1% of total DNA sequences found in the dataset of samples from four sites in the St. Louis River Estuary and all tubercle zones	35

List of Figures

Figure 1. Photo of corroded steel at the DM&IR ore docks exposed during low water levels during 2007 and photo of the top view of a corrosion tubercle on a steel coupon that was retrieved after exposure in the St. Louis River Estuary 4

Figure 2. Schematic diagram of the cathodic depolarization theory (or differential aeration cell model) of pitting corrosion 6

Figure 3. Map of sites where steel coupons were placed on steel structures in the St. Louis River Estuary 9

Figure 4. Cross sectional diagram of a tubercle labeled with zones sampled in this study 17

Figure 5. Average corrosion pit depths on steel coupons after 0.8 and 6.6 years of exposure to water at four sites in the St. Louis River Estuary 23

Figure 6. Microelectrode measurements of dissolved oxygen and ferrous iron concentrations above and within tubercles on experimental steel coupons exposed to water at four sites in the St. Louis River Estuary for 0.8 and 6.6 years 26

Figure 7. Non-metric multidimensional scaling ordinations based on bacterial community DNA sequences that demonstrate differences between bacterial communities in different regions on corroding steel coupons exposed at DSPA Berth 4 in the St. Louis River Estuary 29

Figure 8. Analysis of similarity between bacterial community DNA samples from different tubercle zones at four sites in the St. Louis River Estuary after 0.8 and 6.6 years of exposure to the water 31

Figure 9. Relative abundances of bacterial families containing bacteria that oxidize and reduce iron and sulfur compounds at four sites in the St. Louis River Estuary after 0.8 and 6.6 years of exposure 37

Figure 10. The corrosion rates (mm/yr) for *in situ* and experimental steel coupons versus the service life of the structure or the exposure duration of the coupons (years) in the St. Louis River Estuary 42

List of Abbreviations

Full Title	Abbreviation
Duluth-Superior Harbor	DSH
Duluth Seaway Port Authority	DSPA
Microbiologically influenced corrosion	MIC
Saint Louis River Estuary	SLRE
Iron-oxidizing bacteria	IOB
Iron-reducing bacteria	IRB
Sulfate-reducing bacteria	SRB
Sulfur-oxidizing bacteria	SOB
Larson-Skold Index	LSI

Introduction

The economies of port cities in the Laurentian Great Lakes region are heavily dependent on the maritime shipping industry. Over 226,800 jobs have been created this industry, paying 14.1 billion dollars in wages annually (Martin Associates 2011). Structural integrity of the steel port infrastructure is critical for the continued success of maritime transport in the region. In recent decades, the rate of corrosion in the Duluth-Superior Harbor (DSH) appears to be more aggressive than previously observed (Ray et al. 2009); the loss of steel in this harbor may be 2 to 12 times greater than in other similar freshwater environments (Bushman and Associates 2006, Oster 2012). The aggressive rates of corrosion suggest there is some accelerating process acting on the steel, such as microbiologically influenced corrosion (MIC; Bushman and Associates 2006).

In previous lab and field studies by Oster (2012), a long-term data set was analyzed to determine if differences or long-term changes in water quality were associated with the accelerated corrosion observed. The Larson-Skold Index was used to describe the corrosivity of water toward steel based on the corrosive effects of sulfate and chloride ions and the protective effects of alkalinity (Larson and Skold 1958). This index indicated a low risk of corrosion at 14 of 15 sites where these ion concentrations were measured and historic data at three sites indicate that the Larson-Skold Index has decreased or remained the same over time (Oster 2012). These results indicate that water quality alone does not explain the accelerated corrosion in this harbor.

Corroding steel pilings in the Duluth-Superior Harbor have a rusty appearance with orange, blister-like, raised tubercles on the surface (Figure 1; Ray et al. 2010). These tubercles vary in size from a few millimeters to several centimeters in diameter and pitting corrosion is often observed underneath the tubercles. The appearance of these corroded pilings is consistent with corrosion caused by iron-oxidizing bacteria (IOB; Hamilton 1985). The dark material and sulfidic odor underneath tubercle caps observed in this harbor indicate the presence of sulfate-reducing bacteria (SRB), which have also been widely associated with steel corrosion (Hamilton 1985).

Bostrom (2010) found that steel in both the harbor and laboratory microcosms is covered with complex biofilms containing bacteria from genera associated with MIC. Terminal restriction fragment length polymorphism analysis indicated that bacterial communities at two sites most affected by corrosion were different from communities on sheet steel pilings at the harbor entry where corrosion was minimal. This bacterial community DNA analysis also indicated that microbial communities were different on corrosion tubercles and adjacent areas on the same corroding structure (Hicks 2009).

One proposed mechanism to explain the accelerated corrosion observed under tubercles is the differential aeration cell model, also known as the cathodic depolarization theory (Figure 2; Iverson 1966, Maier et al. 2009, Madigan et al. 2015). This model predicts a gradient of oxygen concentrations decreasing within tubercles to anoxic conditions at the steel surface. The model also predicts stratified bacterial communities

with IOB in outer regions of tubercles and SRB found deeper in corrosion pits in the steel. The metabolism of SRB converts sulfate to sulfide and the sulfide then reacts with ferrous iron to form iron sulfide precipitates. The reaction of ferrous iron drives the anodic reaction of elemental iron to ferrous iron forward. The anodic reaction releases electrons that are consumed in the cathodic reaction outside the tubercle. The conversion of elemental iron to ferrous iron and electrons followed by removal of the free ferrous iron from the metal surface is the principle step in metal loss by corrosion.

Since the harbor water chemistry does not indicate high risk for corrosion and bacterial groups previously associated with corrosion have been observed on steel structures in the Duluth-Superior Harbor, the microenvironments and diverse bacterial metabolisms within corrosion tubercles appear to be involved in the severe corrosion observed in this harbor. Much remains unknown about the microbial community structure and chemical conditions in the near-surface environment where corrosion is taking place. Characterization of these near-surface chemical gradients and spatial distribution of microbial communities is necessary to better understand the accelerated corrosion process and to inform the development of effective mitigation strategies. The study described here links direct measurements of water chemistry and near surface chemical concentrations with bacterial community composition data to provide an extensive, fine-scale description of corrosion tubercles observed on corroding steel surfaces in the Duluth-Superior Harbor.

Figure 1. Left image - Corroded sheet steel at the DM&IR ore docks near Hallett Dock 5, which was exposed in the Duluth-Superior Harbor during low water levels in 2007 (Gene Clark, WI Sea Grant). Right image - Top view of a corrosion tubercle on a steel coupon that was retrieved after exposure in the Duluth-Superior Harbor (Ricky Ray, Naval Research Laboratory, Stennis Space Center).


1 cm

Figure 2. Schematic diagram of the cathodic depolarization theory (differential aeration cell model) of biocorrosion (from Maier et al. 2009). Outer edge of the tubercle is inhabited by iron-oxidizing bacteria while sulfate-reducing bacteria inhabit the corrosion pit near the metal surface. Iron-oxidizing bacteria use ferrous iron and release iron hydroxides and sulfate-reducing bacteria convert sulfate to sulfide. Iron sulfide (FeS) is spontaneously formed chemically from sulfide and ferrous iron ions. A galvanic cell forms and pitting corrosion occurs.

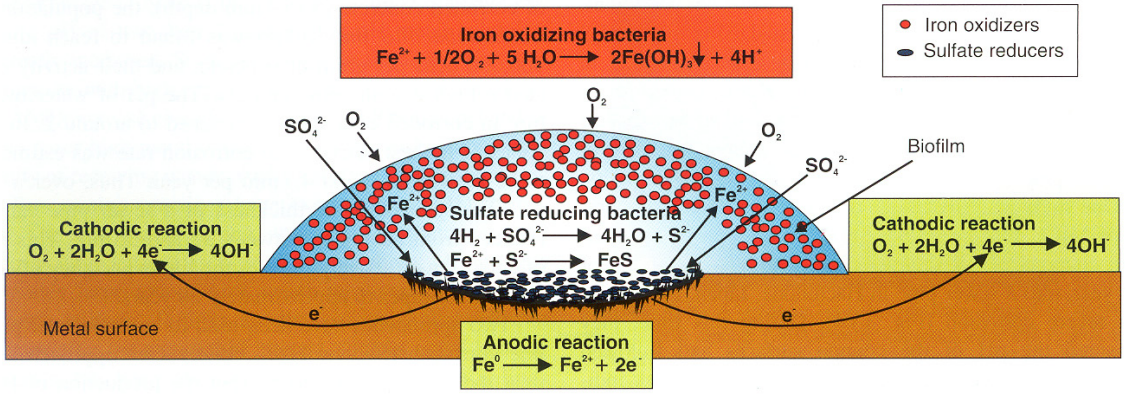
Iron oxidizing bacteria
$Fe^{2+} + 1/2O_2 + 5\ H_2O \rightarrow 2Fe(OH)_3\downarrow + 4H^+$
Iron oxidizers
Sulfate reducers
O_2
SO_4^{2-}
O_2
O_2
SO_4^{2-}
Biofilm
Fe^{2+}
Fe^{2+}
Sulfate reducing bacteria
$4H_2 + SO_4^{2-} \rightarrow 4H_2O + S^{2-}$
$Fe^{2+} + S^{2-} \rightarrow FeS$
Cathodic reaction
$O_2 + 2H_2O + 4e^- \rightarrow 4OH^-$
Cathodic reaction
$O_2 + 2H_2O + 4e^- \rightarrow 4OH^-$
e^-
e^-
Metal surface
Anodic reaction
$Fe^0 \rightarrow Fe^{2+} + 2e^-$

Methods

Site locations and sample collection

Steel coupons (19.1 cm × 11.7 cm × 1.25 cm) were cut from cold rolled sheet steel (ASTM A328, a low carbon steel identical to that used in the construction of about 90% of the structures in the DSH) and placed by a hard-hat diver from AMI Consulting Engineers (Superior, WI) into steel sample trays welded to the adjacent steel structures 1 meter below the water surface. Each coupon was fitted with high-density polyethylene spacers in the rack to electrically isolate the coupons. In late 2006, three coupons were placed at Duluth Seaway Port Authority (DSPA) Berth 4 (Oct. 17), Midwest Energy (Oct. 17), Hallett Dock 5 (Oct 17), and Oliver Bridge (Oct 4). On August 20, 2012, three additional coupons were placed at each of the sites. These sites are located throughout the Duluth-Superior Harbor and in the St. Louis River Estuary (SLRE, Figure 3).

Coupons were recovered from Oliver Bridge and Hallett Dock 5 on June 12, 2013. Three coupons with 6.6 years of exposure in the harbor and three with 0.8 years of exposure were recovered from each site. Coupons were recovered from Midwest Energy and DSPA Berth 4 on June 26, 2013. Two coupons with 6.6 years of exposure and 3 coupons with 0.8 years of exposure were recovered from DSPA Berth 4 and 3 coupons with 0.8 years of exposure were recovered from Midwest Energy. Coupons were collected from the sample trays by a hard-hat diver (AMI Consulting Engineers, Superior, WI) and placed in site water in individual plastic containers. The coupons were transported to the lab in coolers and stored at 4°C before analyses.

Figure 3. Map of sites where steel sample coupons were placed on steel structures in the Duluth-Superior Harbor near Duluth, MN. The harbor is in the St. Louis River Estuary at the confluence of the St. Louis River and Lake Superior. DSPA Berth 4, Midwest Energy and Hallett Dock 5 are shipping docks located within the harbor and the Oliver Bridge site is in the upper St. Louis River Estuary.

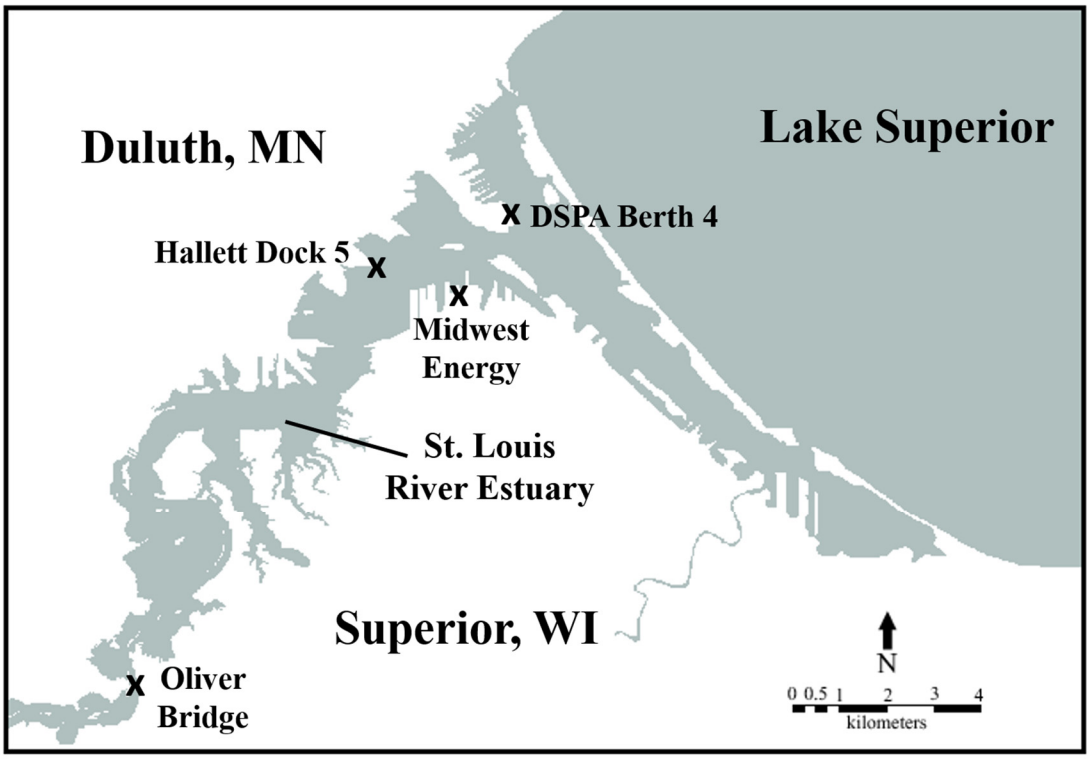
Duluth, MN
Lake Superior
DSPA Berth 4
Hallett Dock 5
Midwest
Energy
St. Louis
River Estuary
Superior, WI
Oliver
Bridge
N
0 0.5 1 2 3 4
kilometers

Bulk water samples were collected adjacent to the steel structures in 1 liter Nalgene polypropylene bottles that had been washed, rinsed with 10% hydrochloric acid and then rinsed with Milli-Q water. Water samples were stored on ice in the field and at 4°C in the laboratory until being sent to Trace Analytical Laboratories, Inc. (Muskegon, MI) for chemical analysis. Additional water from each site was collected in 20-liter polyethylene carboys for later use during the microelectrode analysis.

Water chemistry

Water samples were taken from the Oliver Bridge and Hallett Dock 5 sites on June 12, 2013 and from the Midwest Energy and DSPA Berth 4 sites on June 26, 2013. Water samples from each site were shipped on ice to Trace Analytical Laboratories, Inc. (Muskegon, MI) and analyzed for total copper (EPA Method 6020), chloride (EPA Method 300.0 rev 2.1), sulfate (EPA Method 300.0 rev 2.1) and total alkalinity (SM 2320 B-97).

The Larson-Skold Index of corrosivity was calculated for each site based on the water chemistry analyses. The Larson-Skold Index (Larson and Skold 1958) is a ratio used to describe the corrosivity of water toward mild steel based on the corrosive effects of chloride and sulfate and the protective effect of alkalinity (expressed as $CaCO_3$), all expressed in milliequivalents (mEq). The formula for the index is: (mEq Cl^- + mEq $SO4^{2-}$) / (mEq $CaCO_3$).

Corrosion pit depths

One coupon of each exposure duration from each site was submerged in site water, sealed in water-tight plexiglass containers and shipped overnight on ice to the Naval Research Laboratory, Stennis Space Center. Coupons were cleaned with a solution of hydrochloric acid and distilled water (1:1) with 3.5 g/L of hexamethylene-tetramine. Pit surface profiles were collected from five locations (25 mm x 25 mm) on each of the coupons using a Microphotonics Nanovea PS50 non-contact optical profiler with a 3.5 mm optical laser pen (Ray et al. 2009, 2010). Five pit depths were collected from each of the five profiles for a total of 25 pit depth measurements per coupon. Two way t-tests and ANOVA were used to compare average pit depths and corrosion rates at different sites and exposure durations. Corrosion rates at each site were calculated by dividing the average pit depth by the number of years of exposure in the estuary.

Microelectrode analyses

Voltammetric measurements were made using a DLK-70 Web Pstat electrochemical analyzer (Analytical Instrument Systems, Inc., Ringoes, NJ) and solid state Au/Hg electrodes fabricated using methods described by Brendel and Luther (1995). Electrodes were sanded and polished using 600 grit sand paper and 15, 6, 1 and 0.25 micron diamond polishing compounds (Buehler, Lake Bluff, IL) and lubricated in MetaDi Fluid (Buehler, Lake Bluff, IL). Each electrode was plated with mercury and stored in DI water (Himmelheber et al. 2008).

Microelectrodes were calibrated for both dissolved oxygen and ferrous iron measurements (Himmelheber et al. 2008). Calibration measurements for oxygen were taken at full saturation at laboratory temperature and anoxic conditions. A seven-point calibration curve for ferrous iron was made using concentrations between 0 and 5000 μM. Calibration measurements were made using dilutions of a 300 mM stock of ferrous chloride tetrahydrate (Fisher Scientific, Fair Lawn, NJ) in 0.05% concentrated HCl.

Microelectrode measurements were made on two individual tubercles on a single coupon from each site. Water from each site in the DSH was used to cover coupons before microelectrode measurements were made. Oxygenated site water was filtered through glass fiber prefilters (Millipore, Billerica, MA) to increase clarity and poured back over the coupons. Submerged coupons sat with motionless overlaying water conditions for a minimum of one hour to allow chemical gradients to reestablish. Electrodes were positioned above tubercles using a micromanipulator (World Precision Instruments, Sarasota, FL). Oxygen measurements were recorded at approximately millimeter increments down to the surface of each tubercles. Coupons were stored in filtered site water 4°C between measurements.

To make ferrous iron measurements within corrosion tubercles, filtered water from each site was first degassed by bubbling with N_2 gas overnight through a diffuser. Water overlying the coupons was then poured off and replaced with degassed water from

the appropriate site. The headspace in the containers were kept anoxic using oxygen free N_2 gas. Each coupon sat for a minimum of one hour before a small hole was created in the surface of a tubercle by carefully puncturing with an 18 gauge needle (Sherwood Medical, St. Louis, MO). The electrode was inserted through the needle bore and ferrous iron measurements were made inside the tubercle in approximately millimeter increments toward the steel surface. The process of puncturing the tubercle and taking ferrous iron measurements was repeated for the same two tubercles that were used for oxygen measurements on each coupon.

The microelectrodes were reconditioned between measurements by applying a potential to the electrode to remove electroactive species that may have adhered to the surface. Oxygen measurements were collected using linear sweep voltammetry and ferrous iron was measured using square wave voltammetry as described by Brendel and Luther (1995). Concentrations of oxygen and ferrous iron were calculated from the maximum measured current at -0.75V and the maximum measured current between -1.35V and -1.26V, respectively. Chemical concentrations were determined using linear interpolation from the calibration curves.

Microbial community sampling and analysis

Replicate coupons from each site were designated for microbe sampling (N=2 or 3), microelectrode analysis (N=1) or pit depth analysis (N=1). First, microbial samples were collected from all coupons available from each site, though the most extensive

sampling occurred on those designated entirely to microbe sampling. On sets of coupons with 6.6 years of exposure, microbial samples were taken from four distinct quadrants on the coupon dedicated to microbe sampling and one quadrant each from the single coupons designated for microelectrode and pit depth analyses. There were not enough tubercles on coupons with 0.8 years of exposure to sample separate quadrants within coupons. Therefore, a single composite sample was collected from the coupon designated to microbe sampling and a second composite sample was made from quadrants sampled on the coupons designated for microelectrode and pit depth analyses. Microbial samples were taken from the side of the coupon that was exposed to the harbor.

Microbial samples were collected with two sterile cotton swabs and suspended in phosphate buffered saline (PBS). The PBS solution was then filtered under vacuum onto a Duropore membrane filter (Millipore Corp., 47 mm diameter, 0.22 μm pore size) to collect microbial cells. On each coupon, microbial samples were collected from a non-tubercle area of the steel and from three distinct tubercle zones: the outer surface of tubercles, the underside of tubercle caps and corrosion pits beneath tubercles (Figure 4). Samples from non-tubercle areas and the outer surfaces of tubercles were taken first. Then, the tubercle caps were chipped off the steel and flipped over using sterilized stainless steel spatulas and forceps before collecting microbial samples from the underside of tubercles and corrosion pits.

The membrane filters containing microbial samples from different regions of the

corrosion tubercles were cut into pieces approximately 10 mm^2 using sterilized forceps and scissors. Then, total DNA was extracted from each microbial sample with UltraClean™ Soil DNA extraction kits (Mo Bio Laboratories, Solana Beach, CA, USA) according to the provided manufacturer's instructions. Extracted DNA concentrations were measured using a NanoDrop 1000 Spectrophotometer (ThermoFisher Scientific, Wilmington, DE). DNA was stored at -20° C until PCR amplification.

DNA samples were amplified in triplicate using primers (967F and 1046R) that flank the V6 hypervariable region of the 16S rRNA gene (Sogin et al. 2006, Chakravorty et al. 2007). Amplification was performed on a DNA Engine PTC-200 (Bio-Rad, Hercules, CA) thermal cycler. Barcoded PCR primers (a 6 bp ID tag on the 5' end of either the forward or reverse primer) were used so that multiple samples could be included in a single Illumina sequencer flow cell lane. The PCR amplification mixture contained 25 μL Amplitaq Gold 360 DNA Polymerase (Life Technologies, Grand Island, NY), 2 μL of each PCR primer (0.2 μM), template DNA (10 ng), and nuclease-free water to bring the total volume to 50 μL. PCR cycling conditions were an initial denaturation at 95°C for 5 min and then 25 cycles of 95°C for 30 s, 55°C for 30 s, and 72°C for 30 s, and a final 60 s extension at 72°C. The products of each PCR reaction were cleaned using a MoBio Ultraclean™ PCR Clean-Up kit (Mo Bio Laboratories, Carlsbad, CA) according to the directions included with the kit. Concentrations of the PCR product were measured with a NanoDrop 1000 Spectrophotometer (ThermoFisher Scientific, Wilmlington, DE).

Figure 4. Cross sectional diagram of a tubercle labeled with zones sampled in this study. The arc represents the crusty tubercle cap, the speckled fill represents the material filling the cap and the black lining in the divot indicates the dark precipitate often found in the corrosion pit beneath a tubercle. The three tubercle associated zones sampled were the outer surface of the tubercle, the underside of the tubercle cap and inside corrosion pits underneath tubercles. The final sampled zone was adjacent, non-tubercle surfaces of the steel coupons.

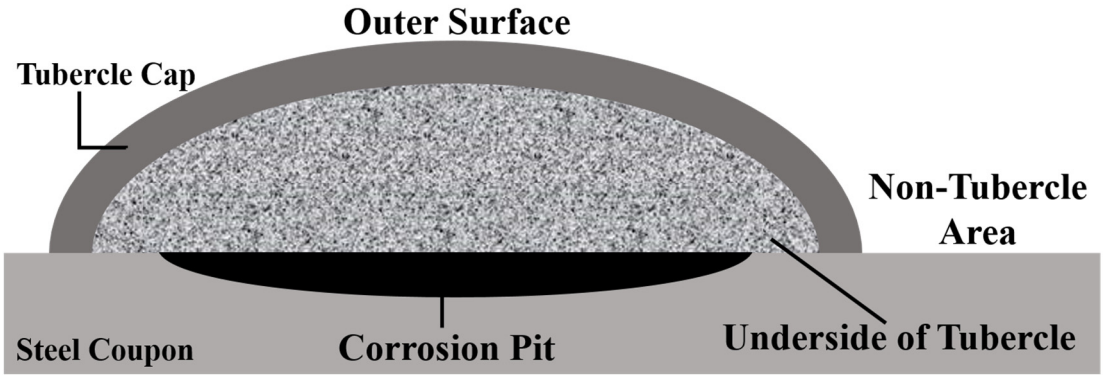
Outer Surface
Tubercle Cap
Non-Tubercle Area
Steel Coupon
Corrosion Pit
Underside of Tubercle

Triplicate PCR products with unique sample barcodes were mixed in equal nanogram quantities to form a single sample for sequencing. These samples were shipped to the University of Minnesota Biomedical Genomics Center on dry ice for sequencing using an Illumina MiSeq sequencer following the manufacturer's protocols (Illumina, Hayward, CA). Sequences from each run were downloaded and stored at the Minnesota Supercomputing Institute. Sequences were obtained as .fastq files and submitted to the National Center for Biotechnology Information Sequence Read Archive. Sequencing results are available through GenBank BioProject PRJNA311760.

Sequence data was processed using the open source software mothur (Schoss et al. 2009) using the methods of Staley et al. (2013). Sequences were first screened for ambiguous bases, homopolymers over 8 bp and more than one mismatch in the primer sequence. Then, singleton sequences were removed and sequences were aligned using the SILVA database (Pruess et al. 2009). Uninformative and misaligned sequences were removed, very similar sequences were clustered and chimeras were removed using the UCHIME algorithm within mothur (Edgar et al. 2011).

To control for the different number of sequence reads in each sample while still capturing as much of the diversity as possible, the number of sequences per sample was normalized by taking a randomly selected subsample of 14,000 sequences. These sequences were clustered into operational taxonomic units (OTUs) at a cutoff value of ≥ 97%. Taxonomy was assigned to OTU consensus sequences using the Ribosomal

Database Project (RDP) taxonomic database. Mothur was also used to generate a Bray-Curtis dissimilarity matrix and calculate coverage (Staley et al. 2013).

Comparisons of microbial communities in different corrosion tubercle regions, coupon sites and exposure periods were made by comparing the number of partial DNA sequences obtained from different bacterial families. Nonmetric multidimensional scaling ordinations were made using the program PC-ORD (MJM Software Designs, Gleneden Beach, OR). Bacterial communities from different samples were compared using ANOSIM, a nonparametric procedure that tests for significant differences between groups, in mothur. The ordinations and ANOSIM analysis were both based on the Bray-Curtis dissimilarity matrices, which quantify the differences in the counts for each taxonomic group. Since the measure of dissimilarity is based on absolute differences between counts, having a large sample size (14,000 sequences per sample) allowed for inclusion of rarer groups in the analyses. Microsoft Excel was used for all other comparisons.

Results

Water chemistry

Chloride, sulfate and alkalinity concentrations results produced Larson-Skold Index values below 0.8 at all sites (Table 1), indicating low corrosivity of the water toward steel. This was consistent with historical index values (Oster 2012). The total (dissolved and particulate) copper concentration in water ranged from 0.0043 to 0.0087 mg/L (Table 1).

Corrosion pit depths

At all sites, average corrosion pit depths were larger on experimental steel coupons after 6.6 years of exposure in the St. Louis River Estuary than on coupons after 0.8 years of exposure (Figure 5; $p<0.0005$). Average pit depths after 6.6 years of exposure ranged from 680 to 1046 μm, while average pit depths ranged from 373 to 540 after 0.8 years of exposure. After 0.8 years, steel coupons at the Midwest Energy and Hallett Dock 5 sites had deeper average corrosion pits (≥ 490 μm) than coupons at the Oliver Bridge and DSPA Berth 4 sites (≤ 422 μm; Figure 5; $p<0.03$). The deepest average corrosion pits (>1,000 μm) were observed on steel coupons from the DSPA Berth 4 site after 6.6 years of exposure (Figure 5; $p<0.0005$). While pits were deeper after longer coupon exposure, average corrosion rates were higher at 0.8 years of exposure (0.467 to 0.676 mm/year) than after 6.6 years of exposure (0.103 to 0.159 mm/year) at every site.

Table 1. Sulfate, chloride, total alkalinity and total copper concentrations measured in water during June 2013 when steel coupons were recovered from four sites in the St. Louis River Estuary. Water samples were collected on June 12, 2013 (Hallett Dock 5 and Oliver Bridge sites) or June 26, 2013 (DSPA Berth 4 and Midwest Energy sites). The Larson-Skold Index was calculated for each site using the sulfate, chloride and total alkalinity measurements. Index values below 0.8 suggest that there is not an increased risk for mild steel corrosion based on the water chemistry.

Site	Sulfate (mg/L)	Chloride (mg/L)	Alkalinity (mg $CaCO_3$/L)	Larson-Skold Index	Total copper (mg/L)
DSPA Berth 4	10	7.7	55	0.23	0.0073
Midwest Energy	7.2	5.2	53	0.17	0.0087
Hallett Dock 5	10	9.1	47	0.30	0.0043
Oliver Bridge	8.5	5.2	43	0.23	0.0053

Figure 5. Average corrosion pit depths on steel coupons after 0.8 and 6.6 years of exposure to water at four sites in the St. Louis River Estuary. Error bars indicate one standard deviation (SD). Unique letters above bars indicate that the mean pit depth was significantly different from all other sites and exposure durations ($p < 0.05$). The number above each bar is the corrosion rate in mm/year.

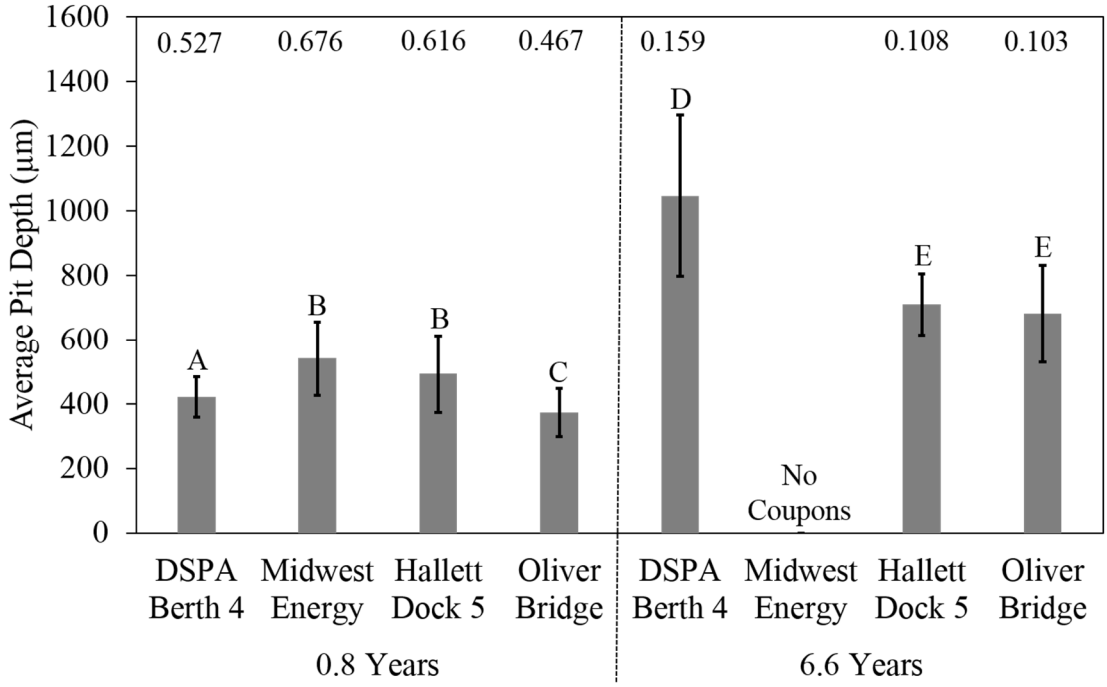
Average Pit Depth (µm)
1600
1400
1200
1000
800
600
400
200
0
0.527
0.676
0.616
0.467
0.159
0.108
0.103
A
B
B
C
D
E
E
No Coupons
DSPA Berth 4
Midwest Energy
Hallett Dock 5
Oliver Bridge
DSPA Berth 4
Midwest Energy
Hallett Dock 5
Oliver Bridge
0.8 Years
6.6 Years

Microelectrode measurements

Oxygen concentrations typically decreased dramatically (often >100-fold decrease) within 5 mm of the outside surface of corrosion tubercles on coupons from all sites and exposures (Figure 6). On several tubercles, the oxygen concentration decreased to near anoxic conditions at the tubercle surface (Figure 6). Ferrous iron concentrations increased with depth into all tubercles (Figure 6). Ferrous iron concentrations typically increased from 0 to 1000-2000 μM within two mm below the top of the tubercle cap, regardless of exposure duration and the site where the coupon was placed. Ferrous iron concentrations within corrosion tubercles on coupons from the Oliver Bridge site were the only exception to this pattern. At this site, ferrous iron concentrations increased from 0 to 2,500 μM or more in the first 2 mm and exceeded 10,000 μM beneath one tubercle cap.

Figure 6. Microelectrode measurements of dissolved oxygen and ferrous iron (Fe^{2+}) concentrations above and within tubercles on experimental steel coupons exposed to water at four sites in the St. Louis River Estuary for 0.8 and 6.6 years. Oxygen measurements for two replicate tubercles are shown with circles connected with solid lines while ferrous iron concentrations inside the same two tubercles are indicated by diamonds connected with dashed lines. Measurements made on one tubercle are shown with open symbols and measurements made on a second tubercle are shown with filled symbols. The tubercle surface is indicated at zero mm and measurements above the tubercle are positive distances while measurements inside the tubercle are negative distances.

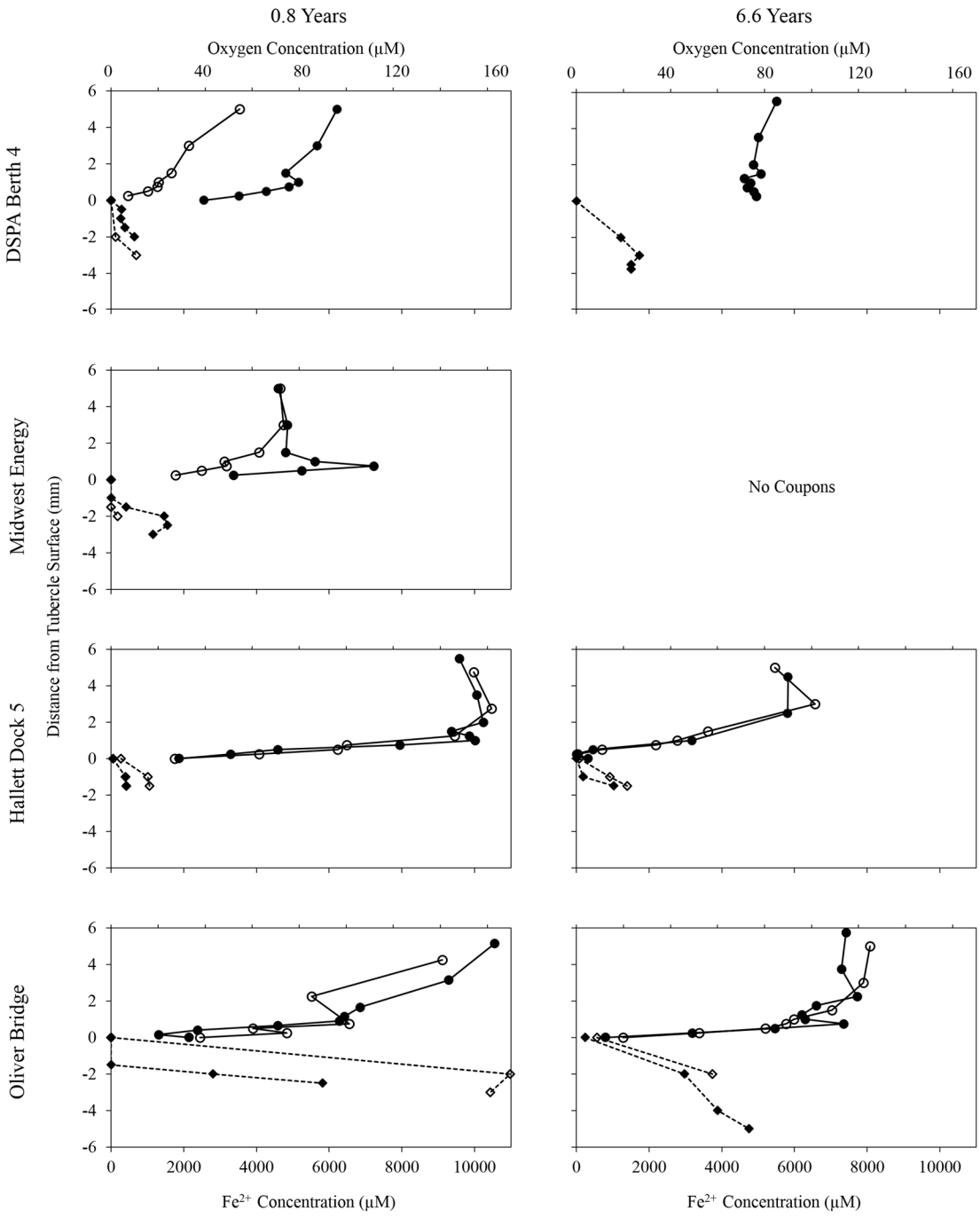
0.8 Years
6.6 Years
Oxygen Concentration (µM)
0
40
80
120
160
DSPA Berth 4
Midwest Energy
Hallett Dock 5
Oliver Bridge
No Coupons
Distance from Tubercle Surface (mm)
6
4
2
0
-2
-4
-6
0
2000
4000
6000
8000
10000
Fe2+ Concentration (µM)

Microbial community differences

Non-metric multidimensional scaling demonstrated that the composition of bacterial communities in various tubercles regions were different. For example, at the DSPA Berth 4 site, bacterial communities on the outer surface of tubercles and the adjacent steel area were distinct from each other after 0.8 years of exposure (Figure 7). They were also different from the overlapping communities on the undersides of tubercle caps and the corrosion pits (Figure 7). After 6.6 years of exposure at this site, the bacterial communities in every tubercle zone were well separated (Figure 7).

Analysis of similarity (ANOSIM) was used to statistically assess the differences observed between bacterial communities in the ordinations (Ramette 2007). Comparisons were made between communities from each tubercle zone, exposure duration and site. Bacterial communities from tubercle zones and the surface of adjacent non-tubercle steel were typically different. The majority of communities were well separated (R values greater than 0.75) but several were separated but overlapping (R values between 0.5 and 0.75). This trend was observed for bacterial communities on corroding steel coupons at all four sites and after both 0.8 and 6.6 years of exposure (Figure 8). The only exceptions were that bacterial communities from on undersides of tubercles were not well separated from those in corrosion pits at DSPA Berth 4 and Oliver Bridge sites after 0.8 years of exposure and at the Hallett Dock 5 site after 6.6 years of exposure. At the Oliver Bridge site, the bacterial community on the outside of corrosion tubercles was not well separated from the community on adjacent non-tubercle steel after 6.6 years of exposure (Figure 8).

Figure 7. Non-metric multidimensional scaling ordinations based on bacterial community DNA sequences that demonstrate differences between bacterial communities in different regions on corroding steel coupons exposed at DSPA Berth 4 in the St. Louis River Estuary. The ordination on the left compares bacterial communities from tubercles on coupons after 0.8 years of exposure to St. Louis River Estuary water, while the ordination on the right compares communities from coupons after 6.6 years of exposure. Individual points are replicate community DNA diversity measurements from tubercle zones on two separate coupons of each age at this site. Overlapping circles indicate that communities from the different tubercle zones are not fully separated.

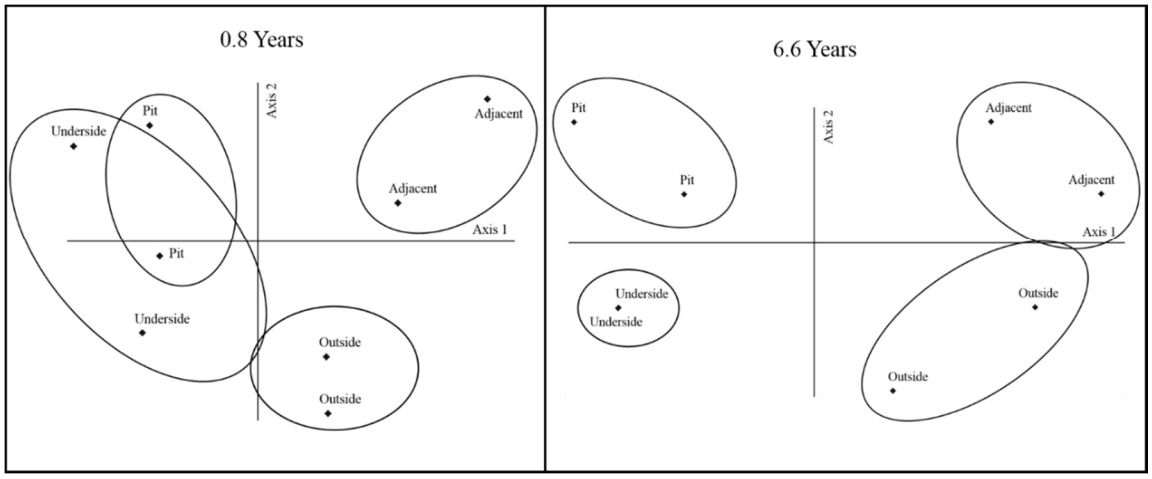
0.8 Years
Axis 2
Axis 1
Pit
Underside
Adjacent
Adjacent
Pit
Underside
Outside
Outside
6.6 Years
Axis 2
Axis 1
Pit
Pit
Adjacent
Adjacent
Underside
Underside
Outside
Outside

Figure 8. Summary of analysis of similarity (ANOSIM) tests between bacterial community DNA sequences from different tubercle zones at four sites in the St. Louis River Estuary after 0.8 and 6.6 years of exposure to St. Louis River Estuary water. Comparisons above the dashed diagonal line are between communities in each tubercle zone after 0.8 years of exposure while comparisons between communities after 6.6 years of exposure are below the diagonal. “S” indicates that the two communities from different tubercle zones were well separated, “S*” indicates that the communities were separated but overlapping and “X” indicates that the communities were not well separated.

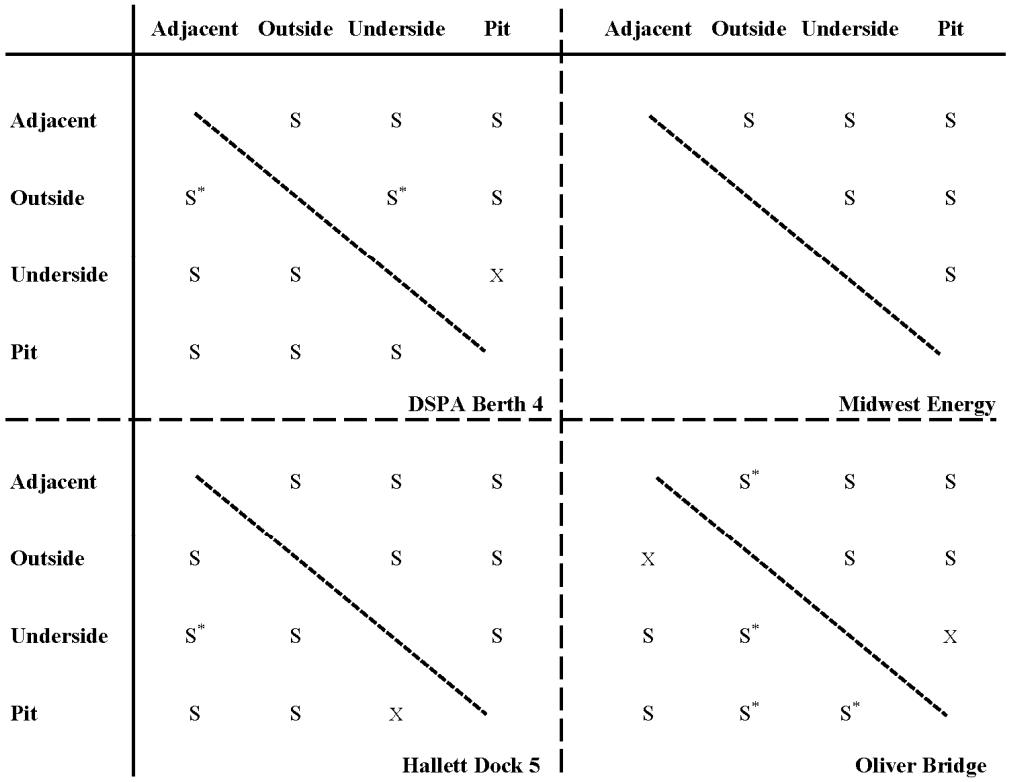
Adjacent
Outside
Underside
Pit
Adjacent
Outside
Underside
Pit
S
S
S
S*
S*
S
S
X
S
S
S
DSPA Berth 4
Midwest Energy
S
S
S
S*
S
S
X
S
S
S*
S
S
S
S*
X
S
S*
S*
Hallett Dock 5
Oliver Bridge

While the ordinations and ANOSIM tests established that bacterial communities were unique in each tubercle zone, those analyses did not provide information about differences in specific bacterial taxa in these zones. Bacterial families identified from the partial 16S rRNA gene sequence analysis in corrosion tubercle zones and on adjacent non-tubercle steel were evaluated to further explore these community differences. The relative abundance of 13 unique bacterial families, estimated from DNA sequence abundances, changed consistently with depth inside the steel corrosion tubercles considering all sites and both exposure durations (Table 2). Many of these bacterial families contain representatives that demonstrate iron-oxidizing (IOB), iron-reducing (IRB), sulfur-oxidizing (SOB), or sulfur/sulfate-reducing (SRB) bacterial metabolism. Families containing SOB and IOB were more abundant on the outside of tubercles and adjacent non-tubercle steel surfaces compared to the underside of tubercles and corrosion pit areas. Inversely, families containing SRB and IRB were more abundant on the underside of tubercles and corrosion pit areas than on the outside of corrosion tubercles or on the surface of non-tubercle steel (Table 2).

Twenty bacterial families each contained at least 1% of the total 16S rRNA gene sequences when data from samples from all tubercle zones, sites, and exposure durations were considered together. Bacterial families with IOB, SOB, IRB and SRB accounted for 15 of the 20 most abundant families (Table 3). Nearly all the most common bacterial families encountered (those responsible for ≥2% of total sequences) with one exception contained bacterial genera that oxidize or reduce sulfur and iron compounds.

Table 2. Bacterial families that had higher relative abundances (estimated from DNA sequence abundance) in different corrosion tubercle zones and adjacent non-tubercle areas on steel coupons. DNA sequences from the bacterial families shown were in higher relative abundance in that zone at every site and both exposure durations. Bacterial families that contain iron-oxidizing (IOB), iron-reducing (IRB), sulfur-oxidizing (SOB) and sulfur-reducing (SRB) taxa are noted.

Location of Greatest Relative Abundance	**Bacterial Family**
Adjacent	Sphingomonadaceae Nitrosomonadaceae Hyphomonadaceae Rhodobacteraceae (IOB)
Outside	Hyphomonadaceae Burkholderaceae (SOB) Rhodobacteraceae (IOB) Acetobacteraceae (SOB and IRB)
Underside	Rhodocyclaceae (IRB and IOB) Holophagaceae (IRB) Geobacteraceae (IRB) Oxalobacteraceae
Pit	Desulfovibrionaceae (IRB and SRB) Oxalobacteraceae Peptococcaceae (IRB and SRB)

Table 3. Bacterial families responsible for at least 1% of the total DNA sequences when data from the four sites in the St. Louis River Estuary and all tubercle zones and both exposure durations were considered. Families containing iron-reducing bacteria (IRB), iron-oxidizing bacteria (IOB), sulfate-reducing bacteria (SRB) or sulfur-oxidizing bacteria (SOB) are indicated by an "X".

Bacterial Family	% of Sequences	IRB	IOB	SRB	SOB
Comamonadaceae	16.19	X			X
Rhodocyclaceae	11.72	X	X		
Burkholderiaceae	5.36				X
Rhodobacteraceae	4.21		X		
Oxalobacteraceae	4.17				
Desulfovibrionaceae	3.68	X		X	
Geobacteraceae	3.55	X			
Peptococcaceae	3.39	X		X	
Acetobacteraceae	2.91	X			X
Nitrospiraceae	2.87		X	X	
Aeromonadaceae	2.38	X			
Sphingomonadaceae	1.86				
Holophagaceae	1.61	X			
Bradyrhizobiaceae	1.53	X			
Xanthomonadaceae	1.34	X			
Neisseriaceae/ Chromobacteriaceae	1.29	X			
Nitrosomonadaceae	1.23				
Pseudomonadaceae	1.22		X		
Hyphomonadaceae	1.18				
Chitinophagaceae	1.07				

Partial 16S rDNA sequences from bacterial families containing IOB were found in all tubercle zones and on adjacent non-tubercle steel from each site. The relative abundance of sequences from IOB-containing families was higher in each tubercle zone on coupons exposed for 0.8 years compared to 6.6 years of exposure (Figure 9). Eleven of the 20 most abundant families contained IRB taxa (Table 3), which led to higher percentages of IRB-containing families than bacterial families containing other iron or sulfur metabolism on coupons at all sites and both exposure durations (Figure 9). The Comamonadaceae was the most abundant bacterial family in the entire sequence dataset. It contains both IRB and SOB members and dominated the trend in the graphs for both IRB and SOB (Figure 9).

DNA sequences from bacterial families containing SRB were more abundant in the corrosion pit zone, accounting for up to 25% of total sequences, relative to the other tubercle zones or adjacent steel (Figure 9). The corrosion pit zone on coupons placed at the Midwest Energy site for 0.8 years also contained a high relative abundance of bacterial DNA sequences from the Peptococcaceae, a bacterial family that has both IRB and SRB representatives. No consistent pattern in relative abundance on adjacent non-tubercle steel was observed within the bacterial families containing IOB, SOB, IRB or SRB (Figure 9).

Figure 9. Relative abundance (based on 16S rDNA sequence analysis) of bacterial families containing iron-reducing bacteria (IRB), iron-oxidizing bacteria (IOB), sulfate-reducing bacteria (SRB) and sulfur-oxidizing bacteria (SOB) on corroding steel coupons at four sites in the St. Louis River Estuary after 0.8 and 6.6 years of exposure. Partial 16S rDNA sequences from bacterial families containing more than one of these physiological groups were included more than one (i.e., appear in multiple graphs). For example, sequences from the Comamonadaceae were included in graphs for both the SOB and IRB bacterial taxa. Different tubercle zones are indicated by bars with different shading. The exact percentage of sequences is included at the top for bars that exceeded the scale of the graph.

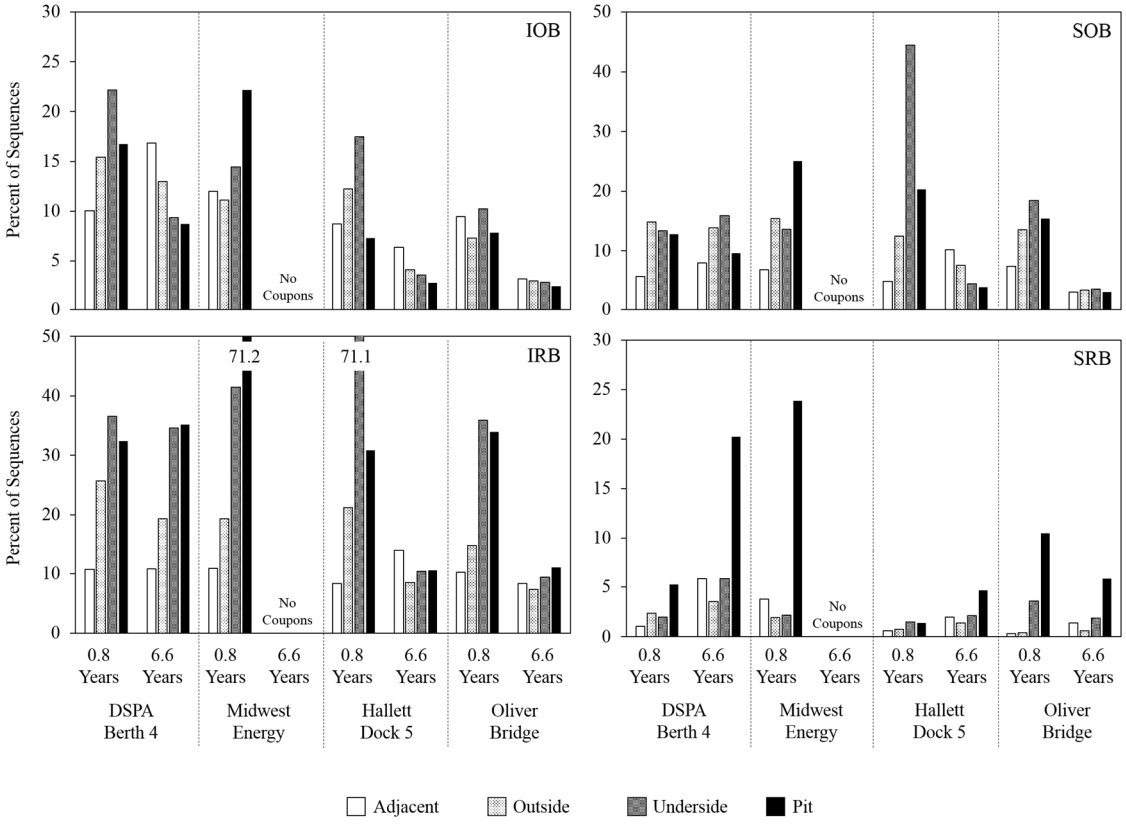
IOB
SOB
IRB
SRB
Percent of Sequences
No Coupons
71.2
71.1
0.8 Years
6.6 Years
DSPA Berth 4
Midwest Energy
Hallett Dock 5
Oliver Bridge
Adjacent
Outside
Underside
Pit

Discussion

Average corrosion rates of steel structures were determined by Oster (2012) for coupons and *in situ* steel structures at many sites in the Duluth-Superior Harbor and St. Louis River Estuary, including the four sites used in this study. He measured corrosion pit depths and calculated average corrosions rates by dividing by the duration that steel coupons or *in situ* structures were exposed in the St. Louis River Estuary (1-4 years for steel coupons; 18-101 years for *in situ* structures). Average corrosion rates were highest in steel coupons after 1 year of exposure and decreased during the next two to three years. Average corrosion rates were lower for *in situ* structures than experimental coupons. Like coupons though, the highest average corrosion rates were observed for *in situ* structures with the least exposure time (18 to 19 years) and lowest after 97 to 101 years of exposure.

Oster's data demonstrated that average corrosion rates were highest during the initial years of exposure and then decreased over time. The trend of decreasing average corrosion rate appeared exponential with a very sharp decline in average corrosion rate over the first five years and then leveling off dramatically after approximately ten years. However, there was a gap in the dataset because it did not include data from any steel coupons or structures with less than one year of exposure or between 4 and 18 years of exposure to water in the St. Louis River Estuary.

The average corrosion rates in this study were calculated using the same method as Oster (2012). The average corrosion rates from this study (Figure 5) filled in some of the gaps in Oster's dataset and were consistent with the trend of average corrosion rates decreasing with age (Figure 10) predicted by Oster (2012). Average corrosion rates calculated for steel coupons after 0.8 years of exposure in this study were higher than rates observed after 1 or more years of exposure. Similarly, average corrosion rates of steel coupons after 6.6 years of exposure were lower than for any coupons in Oster's dataset with less exposure time and filled a gap in the data between steel coupons and *in situ* steel structures in this harbor. These data indicate that steel corrosion is aggressive and occurs very quickly during the first few years of exposure in the DSH but decreases with time.

The Larson-Skold Index values calculated for water in the DSH over several decades (Oster 2012) and in this study have indicated a low risk of corrosion due to the overlying water chemistry. Water chemistry alone does not appear to explain the severe, apparently accelerated, pitting-type corrosion observed on steel structures in the DSH than water quality.

Corrosion rates in laboratory microcosms with bacterial biofilms decrease over time, similar to the trend observed in the DSH (Zhang et al. 2015). Cast iron coupons were exposed to effluent water from a wastewater treatment facility. Biofilms developed on the coupons and accelerated corrosion was observed beneath the biofilms with respect

to the control coupons exposed to sterilized effluent. The corrosion rate was most aggressive during the first stage of the experiment (days 0-7), sharply decreased during the second stage (days 8-15) then decreased gradually through the end of the experiment (30 days). The periods of aggressive, accelerated corrosion followed by a decrease in corrosion rates were more rapid in the laboratory microcosms with cast iron coupons but followed the same trend as the *in situ* coupons and steel structures in the SLRE.

Several models invoking the metabolic activities of bacteria have been proposed to explain accelerated pitting-type corrosion on metal surfaces sometimes observed in aquatic environments. These microbiologically influenced corrosion (MIC) models include the differential aeration cell model (Maier et al. 2009) or cathodic depolarization theory (Iverson 1966, Madigan et al. 2015), and more recently the direct electron transfer theory (Madigan et al. 2015) and copper galvanic couple model (Ray et al. 2009). All of these models require that a biofilm of aerobic bacteria initially develops on a metal surface followed by the establishment of an anoxic zone deeper in the biofilm due to bacterial metabolism, which provides the conditions necessary for the survival and growth of anaerobic bacteria deeper within the biofilm. These models predict chemical gradients and stratified bacterial communities within corrosion tubercles. The chemical and microbiological results from this study are consistent with each of these MIC models but these results do not provide evidence to support one of these models over another.

Figure 10. The corrosion rates (mm/year) for *in situ* steel structures (Oster 2012) and experimental steel coupons (Ray et al. 2009, 2010) versus the service life of the structure or the exposure duration of the coupons (years) in the Duluth-Superior Harbor. Diamonds = 2006 *in situ* steel corrosion rates (Chad Scott, AMI Consulting Engineers); filled circles = experimental steel coupon corrosion rates (Ray et al. 2009); triangles = experimental steel coupon corrosion rates (Ray et al. 2010); squares = 2010 and 2011 *in situ* steel corrosion rates (Oster 2012); open circles = average corrosion rates of steel coupons from this study.

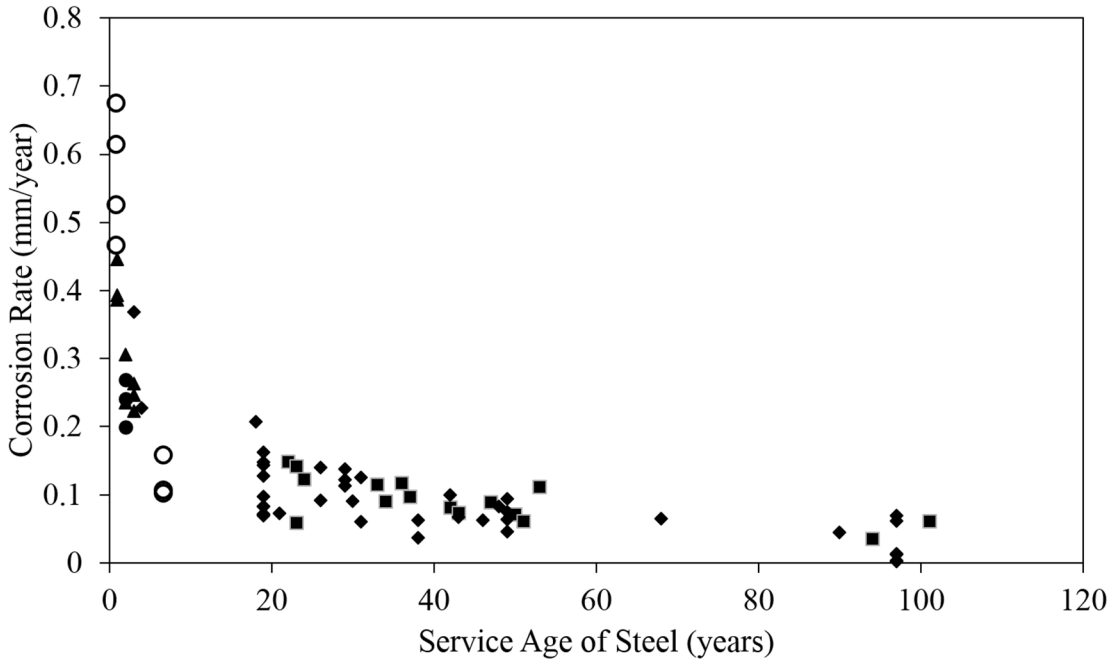
Corrosion Rate (mm/year)
0.8
0.7
0.6
0.5
0.4
0.3
0.2
0.1
0
0
20
40
60
80
100
120
Service Age of Steel (years)

Decreasing oxygen concentrations closer to tubercle surfaces and increasing ferrous iron concentrations measured inside the corrosion tubercles in this study are consistent with predictions of these MIC models. In these models, oxic or microaerophilic conditions near the outside surface of corrosion tubercles provide zones for aerobic microorganisms such as sulfur- and iron-oxidizing bacteria, while an anoxic zone deeper within the tubercles provides the conditions necessary for sulfur- and iron-reducing anaerobic bacteria to flourish.

Initial biofilm formation is complex and impacted by both the surface conditions of the steel and the chemistry of the bulk medium around the steel. In laboratory experiments, Javed et al. (2015) observed SRB cell attachment to steel coupons within the first 60 minutes under all experimental conditions. In microcosms with added ferrous iron, a greater number of SRB cells adhered to the surface and the longer term pitting corrosion was more aggressive than in conditions without supplemental ferrous iron. These observations indicate that SRB can be involved in the early colonization of a corrosion tubercle and that their biological activity can accelerate corrosion in areas with elevated ferrous iron concentrations, such as within a tubercle.

In this study, distinct bacterial communities were observed in different tubercle zones. DNA sequences from bacterial families containing genera that can oxidize iron and sulfur compounds were consistently found on the outsides of tubercles and on non-tubercle steel surfaces. DNA sequences from families containing bacterial genera that can

reduce sulfur and iron compounds were more often found beneath the tubercle surface and in the corrosion pit zone than on the outer surface of tubercles or adjacent non-tubercle steel. DNA sequences from bacterial families containing IOB genera were observed throughout tubercles regardless of the duration steel coupons were exposed in the DSH. However, DNA sequences from bacterial families containing IOB genera were relatively more abundant in 0.8 year old than 6.6 year old corrosion tubercles. DNA sequences from bacterial families harboring SRB were more abundant in the corrosion pit and underside of tubercle zones than on the outer surface of tubercles or the adjacent steel.

The community differences observed over time on steel coupons exposed in the SLRE are consistent with the development of corrosive bacterial biofilms observed in other environments. Rajala et al. (2015) found that native deep groundwater bacterial communities readily colonized steel and caused localized corrosion beneath biofilms. Bacterial community fingerprinting indicated that these communities changed over time and quantitative PCR analysis of the *dsr*B gene revealed a diverse community of SRB after 3 months of incubation (Rajala et al. 2015).

The differential aeration cell and copper galvanic couple models differ in the predicted result of the reducing conditions. In the differential aeration cell model, SRB grow in the anoxic, reducing environment and produce sulfide from sulfate. The sulfide reacts with ferrous iron forming iron sulfide precipitates. The ferrous iron reaction with

sulfide drives the anodic reaction of elemental iron forming ferrous iron forward and localized pitting corrosion occurs (Enning and Garrelfs 2014). There must be a copper source in order for the copper galvanic couple model to work. Water overlying the corrosion tubercles had very low dissolved copper concentrations at each of the DSH sites evaluated. The ASTM A328 steel used to construct the coupons and many of the steel structures in this harbor, however, contains a minimum of 0.20% copper. Once a tubercle has formed and corrosion begins, then the copper in the steel may be released with iron from the metal surface into the corrosion tubercle. Some SRB biofilms are known to accumulate solid copper sulfides (White and Gadd 1999), which may assist the precipitation of copper in the corrosion pits predicted by the copper galvanic couple model. Ray et al. (2009) detected uniform layers of copper under tubercles on similar steel coupons exposed in the DSH. If the copper precipitated in the corrosion pit zone is exposed to oxygen, for example when seasonal ice scouring occurs, then the galvanic current would increase due to the copper, a more noble metal, overlaying the iron in the steel and localized accelerated corrosion might occur.

The cathodic depolarization theory (Figure 1) predicts that the cathodic reaction occurs outside the tubercle where oxygen in the overlaying water removes electrons from the steel surface. Hardy and Brown (1984) observed that exposure to air increased the depth of corrosion pits beneath tubercles in laboratory experiments with SRB cultures and steel coupons. However, the presence of SRB within the tubercle may also facilitate the removal of electrons from the steel surface through multiple metabolic pathways

depending on the carbon sources available (Cord-Ruwisch and Widdel 1986). The direct removal of electrons from the steel surface by bacteria is termed electrical MIC (EMIC) and has been shown to enhance corrosion (Enning et al. 2012, Kato 2016). While this study did not investigate the cathodic reactions occurring, the presence of oxygen measured in the overlaying water and the observed SRB within tubercles allows for either or both of these mechanisms to be contributing to the accelerated corrosion beneath the tubercles.

The sharp chemical gradients observed near in this study allow the development of distinct bacterial communities over very short distances (i.e., mm range) within these corrosion tubercles. The chemical and bacterial DNA sequence data collected in this field experiment were consistent with the initial processes common to all the MIC models. The presence of SRB in the anoxic pits under tubercles is consistent with the differential aeration cell model and may also support the copper galvanic couple model, if SRBs assist copper precipitation in the corrosion pit zone. It is possible that both of these mechanisms (differential aeration cell and copper galvanic couple) are operating at the surface of submerged steel structures in the DSH. This study of steel exposed to water in the DSH has confirmed that corrosion tubercles are complex ecosystems with extreme chemical gradients and characterized microzones with distinct bacterial communities.

References

Bostrom, J. 2010. Microbiological and Chemical Aspects of Corrosion of Sheet Steel in the Duluth-Superior Harbor. Masters Thesis. University of Minnesota.

Brendel, P.J. and G.W. Luther, III. 1995. Development of a Gold Amalgam Voltammetric Microelectrode for the Determination of Dissolved Fe, Mn, O_2, and S(-II) in Porewaters of Marine and Freshwater Sediments. Environ. Sci. Technol. 29:751-761.

Bushman & Associates, Inc. 2006. Linear polarization resistant corrosion rate (mpy). Final report to US Army Corps of Engineers (Detroit District), Detroit, MI.

Chakravorty, S., D. Helb, M. Burday, N. Connell, D. Alland. 2007. A detailed analysis of 16S ribosomal RNA gene segments for the diagnosis of pathogenic bacteria. Journal of Microbiological Methods. 69: 330-339.

Cord-Ruwisch, R. and F. Widdel. 1986. Corroding iron as a hydrogen sources for sulphate reduction in growing cultures of sulphate-reducing bacteria. Applied Microbiology and Biotechnology 25:169-174.

Edgar, R.C., B.J. Haas, J.C. Clemente, C. Quince and R. Knight. 2011. UCHIME improves sensitivity and speed of chimera detection. Bioinformatics. 27(16):2194-2200.

Enning, D., H. Venzlaff, J. Garrelfs, H.T. Dinh, V. Meyer, K. Mayrhofer, A.W. Hassel, M. Stratmann and F. Widdel. 2012. Marine sulfate-reducing bacteria cause serious corrosion of iron under electroconductive biogenic mineral crust. Environmental Microbiology 14(7):1772-1787.

Enning, D. and J. Garrelfs. 2014. Corrosion of iron by sulfate-reducing bacteria: New views of an old problem. Applied and Environmental Biology 80(4):1226-1236.

Hamilton, W.A. 1985. Sulfate-reducing bacteria and anaerobic corrosion. Ann. Rev. Microbiol. 39:195-217.

Hardy, J.A. and J.L. Brown. 1986. The corrosion of mild steel by biogenic sulfide films exposed to air. Corrosion 40(12):650-654.

Hicks, R. E. 2009. Assessing the role of microorganisms in the accelerated corrosion of port transportation infrastructure in the Duluth-Superior Harbor. CURA Reporter 39(1-2):4-10.

Himmelheber, D.W., M. Taillefert, K.D. Pennell and J.B. Hughes. 2008. Spatial and Temporal Evolution of Biogeochemical Processes Following *In Situ* Capping of Contaminated Sediments. Environ. Sci. Technol. 42: 4113-4120.

Iverson, W.P. 1966. Direct Evidence for the Cathodic Depolarization Theory of Bacterial Corrosion. Science 151(3713):986-988.

Javed, M.A., P.R. Stoddart and S.A. Wade. 2015. Corrosion of carbon steel by sulphate reducing bacteria: Initial attachment and the role of ferrous ions. Corrosion Science 93:48-57.

Kato, S. 2016. Microbial extracellular electron transfer and its relevance to iron corrosion. Microbial Biotechnology 9:141-148.

Larson, T.E. and R.V. Skold. 1958. Laboratory studies relating mineral quality of water to corrosion of steel and cast iron. Corrosion 14(6):285-288.

Madigan, M.T., J.M. Martinko, K. S. Bender, D. H. Buckley, and D. A. Stahl. 2015. Brock Biology of Microorganisms, 14th Ed., Pearson Benjamin Cummings, San Francisco, CA.

Maier, R.M., I.L. Pepper, and C. P. Gerba. 2009. Environmental Microbiology, 2nd Ed. Academic Press, Burlington, MA.

Martin Associates. 2011. The Economic Impacts the Great Lakes St. Lawrence Seaway System. October 18, 2011. p 2-9. www.marinedelivers.com.

Oster, R. 2012. Modeling the Corrosive Loss of Port Infrastructure in the Duluth- Superior Harbor and the North Shore of Lake Superior . Masters Thesis. University of Minnesota.

Pruesse, E., C. Quast, K. Knittel, B.M. Fuchs, W.G. Ludwig, J. Peplies, and F.O. Glockner. 2007. SILVA: a comprehensive online resource for quality checked and aligned ribosomal RNA sequence data compatible with ARB. Nucleic Acids Res 35:7188–7196.

Rajala, P., L. Carpen, M. Vepsalainen, M. Raulio, E. Sohlberg and M. Bomberg. 2015. Microbially induced corrosion of carbon steel in deep groundwater environment. Frontiers in Microbiology 6(647):1-12.

Ray, R., J. Lee and B. Little. 2009. Factors Contributing to Corrosion of Steel Pilings in Duluth Superior Harbor. Corrosion 65(11):707-717.

Ray, R.I., J.S. Lee, B.J. Little, and T.L. Gerke. 2010. The anatomy of tubercles: A corrosion study in a fresh water estuary. Materials and Corrosion 61(12):993-999.

Schloss P.D., S.L. Westcott, T. Ryabin, J.R. Hall, M. Hartmann, et al. 2009. Introducing mothur: Open-source, platform-independent, community-supported software for describing and comparing microbial communities. Appl Environ Microbiol 75: 7537–7541.

Sogin M.L., H.G. Morrison, J.A. Huber, D.M. Welch, S.M. Huse, et al. 2006. Microbial diversity in the deep sea and the underexplored "rare biosphere". Proceedings of the National Academy of Sciences 103: 12115-12120.

Staley, C., T. Unno, T.J. Gould, B. Jarvis, J. Philips, J.B. Cotner and M.J. Sadowsky. 2013. Application of Illumina next-generation sequenceing to characterize the bacterial community of the Upper Mississippi River. Journal of Applied Microbiology 115:1147-1158.

White, C. and G.M. Gadd. 2000. Copper accumulation by sulfate-reducing bacterial biofilms. Federation of European Microbiological Studies Microbiology Letters 183:313-318.

Zhang, H., Y. Tian, J. Wan and P. Zhao. 2015. Study of biofilm influenced corrosion on cast iron pipes in reclaimed water. Applied Surface Science 357:236-247.